



Long-term particulate matter modeling for health effect studies in California – Part 2: Concentrations and sources of ultrafine organic aerosols

Jianlin Hu¹, Shantanu Jathar², Hongliang Zhang³, Qi Ying⁴, Shu-Hua Chen⁵, Christopher D. Cappa⁶, and Michael J. Kleeman⁶

¹Jiangsu Key Laboratory of Atmospheric Environment Monitoring and Pollution Control, Jiangsu Engineering Technology Research Center of Environmental Cleaning Materials, Collaborative Innovation Center of Atmospheric Environment and Equipment Technology, School of Environmental Science and Engineering, Nanjing University of Information Science and Technology, 219 Ningliu Road, Nanjing 210044, China

²Department of Mechanical Engineering, Colorado State University, Fort Collins, CO, USA

³Department of Civil and Environmental Engineering, Louisiana State University, Baton Rouge, LA, USA

⁴Zachry Department of Civil Engineering, Texas A&M University, College Station, TX, USA

⁵Department of Land, Air, and Water Resources, University of California, Davis, One Shields Avenue, Davis, CA, USA

⁶Department of Civil and Environmental Engineering, University of California, Davis, One Shields Avenue, Davis, CA, USA

Correspondence to: Jianlin Hu (hu_jianlin@126.com, jianlinhu@nuist.edu.cn) and Michael J. Kleeman (mjkleeman@ucdavis.edu)

Received: 8 October 2016 – Discussion started: 12 December 2016

Revised: 15 March 2017 – Accepted: 22 March 2017 – Published: 26 April 2017

Abstract. Organic aerosol (OA) is a major constituent of ultrafine particulate matter (PM_{0.1}). Recent epidemiological studies have identified associations between PM_{0.1} OA and premature mortality and low birth weight. In this study, the source-oriented UCD/CIT model was used to simulate the concentrations and sources of primary organic aerosols (POA) and secondary organic aerosols (SOA) in PM_{0.1} in California for a 9-year (2000–2008) modeling period with 4 km horizontal resolution to provide more insights about PM_{0.1} OA for health effect studies. As a related quality control, predicted monthly average concentrations of fine particulate matter (PM_{2.5}) total organic carbon at six major urban sites had mean fractional bias of –0.31 to 0.19 and mean fractional errors of 0.4 to 0.59. The predicted ratio of PM_{2.5} SOA / OA was lower than estimates derived from chemical mass balance (CMB) calculations by a factor of 2–3, which suggests the potential effects of processes such as POA volatility, additional SOA formation mechanism, and missing sources. OA in PM_{0.1}, the focus size fraction of this

study, is dominated by POA. Wood smoke is found to be the single biggest source of PM_{0.1} OA in winter in California, while meat cooking, mobile emissions (gasoline and diesel engines), and other anthropogenic sources (mainly solvent usage and waste disposal) are the most important sources in summer. Biogenic emissions are predicted to be the largest PM_{0.1} SOA source, followed by mobile sources and other anthropogenic sources, but these rankings are sensitive to the SOA model used in the calculation. Air pollution control programs aiming to reduce the PM_{0.1} OA concentrations should consider controlling solvent usage, waste disposal, and mobile emissions in California, but these findings should be revisited after the latest science is incorporated into the SOA exposure calculations. The spatial distributions of SOA associated with different sources are not sensitive to the choice of SOA model, although the absolute amount of SOA can change significantly. Therefore, the spatial distributions of PM_{0.1} POA and SOA over the 9-year study period provide

useful information for epidemiological studies to further investigate the associations with health outcomes.

1 Introduction

Organic aerosol (OA) is a significant constituent of fine particulate matter (PM_{2.5}) (Zhang et al., 2007) and a dominant constituent of ultrafine particulate matter (PM_{0.1}) (Kleeman et al., 2009; Sardar et al., 2005b). Epidemiology studies carried out over the past 20 years link PM_{2.5} to severe short-term and long-term health effects such as asthma, cardiorespiratory disease, and lung cancer (Dockery, 2001; Dockery and Pope, 1994; Dockery et al., 1993; Franklin et al., 2007; Le Tertre et al., 2002; Pope and Dockery, 2006; Pope et al., 2002). Epidemiological studies for PM_{0.1} mass are in the early stages of development but preliminary results show associations with premature mortality (Ostro et al., 2015) and low birth weight (Laurent et al., 2014). OA is an important species due to its contribution to PM_{2.5} and PM_{0.1} mass, and the toxicity of some compounds within OA has motivated even greater scrutiny in health studies (Mauderly and Chow, 2008). A few PM_{2.5} epidemiology studies have investigated the associations between exposure to OA and health effects with mixed results (Cao et al., 2012; Krall et al., 2013; Levy et al., 2012; Mar et al., 2000; Ostro et al., 2006, 2010). The early epidemiological studies conducted for PM_{0.1} have identified subcategories of OA that are highly associated with negative health effects (Laurent et al., 2014, 2016a, b; Ostro et al., 2015) and these results merit further investigation to identify the exact sources and compound classes that may be related to PM_{0.1} OA toxicity.

The exposure fields used in the published PM_{0.1} epidemiology studies to date have been generated with chemical transport models (CTMs) because PM_{0.1} measurements with sufficient spatial or temporal resolution are not widely available. In these studies, predictions using the UCD/CIT (University of California Davis/California Institute of Technology) model were evaluated against PM_{2.5} and PM_{0.1} point measurements as a confidence-building exercise and the model predictions were then used to estimate exposure fields with ~4 km and ~24 h resolution over the state of California (Hu et al., 2014a, b, 2015). The OA exposure fields generated through this approach reflect the state-of-the-science predictions from CTMs at the time they were done, but they may not capture the full complexity of atmospheric OA. OA consists of primary organic aerosol (POA) and secondary organic aerosol (SOA). POA is directly emitted to the atmosphere in the particle phase and SOA is formed in the atmosphere from the oxidation of volatile or semivolatile organic compounds (Seinfeld and Pankow, 2003). Both POA and the precursors of SOA can be emitted from anthropogenic and biogenic sources (Mauderly and Chow, 2008). Numerous theories have been put forward about the volatility of

POA (Robinson et al., 2007), the conversion of intermediate-volatility compounds to SOA (Jathar et al., 2014; Zhao et al., 2014), and the role of water in SOA formation (Jathar et al., 2016; Pankow et al., 2015). A comprehensive model for OA that has been fully constrained by measurements has not been demonstrated to date, which makes it difficult to estimate PM_{2.5} OA exposure using CTMs. However, measurements indicate that the OA in the PM_{0.1} size fraction is more heavily influenced by POA (Ham and Kleeman, 2011; Kleeman et al., 2009), which makes estimating exposure to PM_{0.1} using CTMs more feasible.

The current paper, as the fourth in the series (Hu et al., 2014a, b, 2015), investigates the UCD/CIT model capability in predicting the concentrations and sources of POA and SOA in PM_{0.1}. The objective of this study is to identify the features of the CTM POA and SOA results that could add skill to the exposure assessment for epidemiological studies and to discuss the potential problems in modeling POA and SOA for use in health effect studies.

2 Methods

2.1 Model description

The source-oriented UCD/CIT air quality model was used to predict OA concentrations in the current study. The UCD/CIT model tracks primary particles and SOA formation from different sources separately through the calculation of all major aerosol processes such as emissions, transport, deposition, gas-to-particle conversion, and coagulation. The standard algorithms of these processes used in the current study are provided in a companion paper (Hu et al., 2015) and references therein, and so only the details of the algorithms for POA and SOA source apportionment calculation are described here.

The UCD/CIT source-oriented air quality model tracks primary particles emitted from different sources by adding artificial tracers to represent total primary mass contributions from different sources in each particle size bin (Ying et al., 2008). The emissions of tracers are empirically set to be 1 % of the total mass of primary particles emitted from each source category, and thus the particle radius and the dry deposition rate are not significantly changed. The primary PM total mass concentrations from a given source then are directly correlated with the simulated artificial tracer concentrations from that source. Source-specific emission profiles are used to estimate the POA concentrations in the primary PM total mass using the Eq. (1):

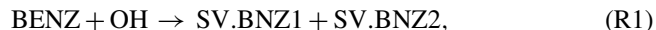
$$\text{POA}_{i,j} = C_{i,j} \times A_{i,j}, \quad (1)$$

where $\text{POA}_{i,j}$ and $C_{i,j}$ represent POA concentration and primary PM total mass concentration in size bin i from j th source, respectively. $A_{i,j}$ represents OA fraction per unit mass of PM emitted from the j th emission source in size

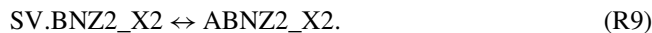
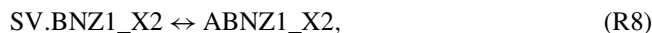
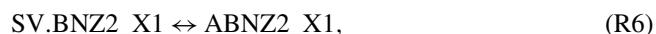
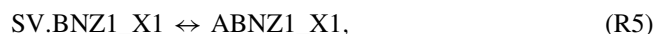
bin *i*. More details describing the POA source apportionment technique and the emission profiles are provided in the previous studies (Ying and Kleeman, 2004; Ying et al., 2008).

The SOA module used in the current study follows the two-product method described by Carlton et al. (2010). SOA formation is considered from seven precursors: isoprene, monoterpenes, sesquiterpenes, long-chain alkanes, high-yield aromatics, low-yield aromatics, and benzene. The seven precursors form 12 semivolatile products and seven nonvolatile products. The calculations consider dynamic gas-particle conversion of the semivolatile and nonvolatile products. A more detailed description of the SOA module and parameters used in gas-to-particle transfer calculation is provided in Part 1 (Hu et al., 2015) and references therein.

The original SOA module described above was modified to have the source apportionment capability inherent in the UCD/CIT model. SOA source apportionment is predicted by tracking the SOA precursor emissions from different sources individually through all atmospheric processes as they react to form low-volatility products that can partition to the particle phase based on the SOA module described above. This approach was initially developed for source apportionment of secondary inorganic aerosols, such as nitrate, sulfate, and ammonium (Mysliwiec and Kleeman, 2002; Ying and Kleeman, 2006). Later, this approach was applied for SOA source apportionment in California using the Caltech Atmospheric Chemistry Mechanism (Chen et al., 2010; Kleeman et al., 2007) and in Texas using the SAPRC99 mechanism (Zhang and Ying, 2011). In the current study, the SAPRC11 mechanism was used and expanded to track the reactions of SOA precursors emitted from different sources. Chemical reaction products leading to SOA formation are labeled with the source identity of the reactant so that source attribution information is preserved. For the example of benzene (BENZ) reaction with OH forming benzene-derived SOA,



where SV.BNZ1 and SV.BNZ2 represent the two semivolatile products that partition between gas and particle phase, and ABNZ1 and ABNZ2 represent the particle-phase SOA products from SV.BNZ1 and SV.BNZ2, respectively. If there are two sources for BENZ, then BENZ is expanded into two species BENZ_X1 and BENZ_X2 in the model. The above pathways (Reactions 1–3) are then expanded as



Thus, the SOA products from BENZ (i.e., ABNZ1_X1, ABNZ1_X2, ABNZ2_X1, and ABNZ2_X2) contain the information needed to calculate source contributions to the SOA concentrations.

2.2 Model application

The UCD/CIT model was applied to simulate the concentrations and sources of POA and SOA during ~a decadal period (9 years from 1 January 2000 to 31 December 2008) over California using a one-way nesting technique added to the UCD/CIT model (Zhang and Ying, 2010). The parent domain covers the entire state of California using a 24 km horizontal grid resolution and two nested domains cover the most populated areas (>92 % of California total population) using a 4 km horizontal grid resolution. A detailed description of the emissions inventory used for the analysis has been presented previously (Hu et al., 2015) and so only a brief summary is discussed in the current paper. Emissions of the seven SOA precursors were grouped into nine source categories: on-road gasoline engines, off-road gasoline engines, on-road diesel engines, off-road diesel engines, wood smoke, meat cooking, high-sulfur fuel combustion, other anthropogenic sources (solvent usage, waste disposal emissions, etc.), and the natural/biogenic sources. Primary PM emissions were also grouped into these nine source categories. Particulate composition, number, and mass concentrations in the range between 0.01 and 10 μm in diameter were represented in 15 size bins with the first 5 bins for PM_{0.1} (0.01 to 0.1 μm) in the model. Biogenic emissions were generated using the US EPA's biogenic emission inventory system (BEIS3.14). Sea salt emissions were estimated based on wind speed as described in Part 1 (Hu et al., 2015). The Weather Research and Forecasting model (WRF) v3.1.1 (William et al., 2008) was used to simulate the 24 and 4 km hourly meteorological fields (wind, temperature, humidity, precipitation, radiation, air density, and mixing layer height) that drove the UCD/CIT model simulations. WRF simulations were initialized and bounded by the North American Regional Reanalysis (NARR) data with 32 km resolution and 3 h time resolution. The four-dimensional data assimilation (FDDA) (Liu et al., 2005) technique was used and the surface friction velocity (u^*) in the WRF model was increased by 50 % to improve the surface wind predictions as suggested by previous studies (Hu et al., 2010, 2012; C. F. Mass, University of Washington, personal communication, 2010). Details of the modeling domains, vertical cell spacing, preparation of emissions, and meteorological inputs (including a full comparison to meteorological measurements) are provided in Part I of the series (Hu et al., 2015).

3 Results

3.1 Concentrations of POA and SOA

Hourly POA and SOA concentrations in multiple size fractions were calculated throughout the 9-year simulation period and then averaged to daily and monthly average concentrations. Although the focus of the current study is $PM_{0.1}$ POA and SOA, the predicted $PM_{2.5}$ OA concentrations were also calculated and compared to measurements as a confidence-building exercise (since $PM_{0.1}$ measurements are not routinely available). Model calculations predict organic matter (OM) concentrations while ambient measurements quantify organic carbon (OC) concentrations. Simulated OM concentrations are converted to OC concentrations using an OM/OC ratio of 1.6 for POA (Turpin and Lim, 2010) and species-specific OM/OC ratios for SOA species taken from Table 1 in Carlton et al. (2010). Detailed evaluation of the model performance for $PM_{2.5}$ OC (and other $PM/gaseous$ species) has been presented in the first paper in the series (Hu et al., 2015). In summary, predicted monthly average $PM_{2.5}$ OC has a mean fractional bias (MFB) of -0.32 and a mean fractional error (MFE) of 0.43 . Monthly MFB and MFE (Eqs. S1 and S2 in the Supplement) calculated using daily average OC generally meet the model performance criteria proposed by Boylan and Russell (2006) (Eqs. S3 and S4).

Figure 1 illustrates the time series of the predicted and measured monthly average total $PM_{2.5}$ OC concentrations at seven major urban locations: (a) Sacramento, (b) San Jose, (c) Fresno, (d) Bakersfield, (e) Los Angeles, (f) Riverside, and (g) El Cajon. At each site, daily average measured concentrations of the $PM_{2.5}$ total mass and OC were obtained from California Air Resources Board (CARB) (CARB, 2011) “1 in 3” sampling network and averaged over the 9-year period. Measured $PM_{2.5}$ OC concentrations at all sites show strong seasonal variation with higher concentrations in winter months and lower concentrations in summer months. OC concentrations predicted by the UCD/CIT model generally capture the monthly average concentrations and seasonal variations with MFB ranging from -0.31 to 0.19 and MFE ranging from 0.4 to 0.59 . However, the model predicts much weaker trends of $PM_{2.5}$ OC over the 9 years at Los Angeles and Riverside, indicating that the declining emission trends might not be well represented in the inventory. At Sacramento and Fresno, the measured monthly average OC concentrations frequently exceeded $10 \mu\text{g m}^{-3}$ in winter and the maximum monthly OC concentrations reached or exceeded $\sim 25 \mu\text{g m}^{-3}$. Wood smoke is predicted to be the dominant OC source in winter at the two locations, contributing over 70% of the total OC concentrations on average. Wood smoke is also predicted to be the dominant OC source in winter at San Jose and Bakersfield. Model calculations tend to overpredict the winter OC concentrations at San Jose, indicating that the wood smoke emissions are likely overestimated in this area. This is consistent with more recent surveys of home

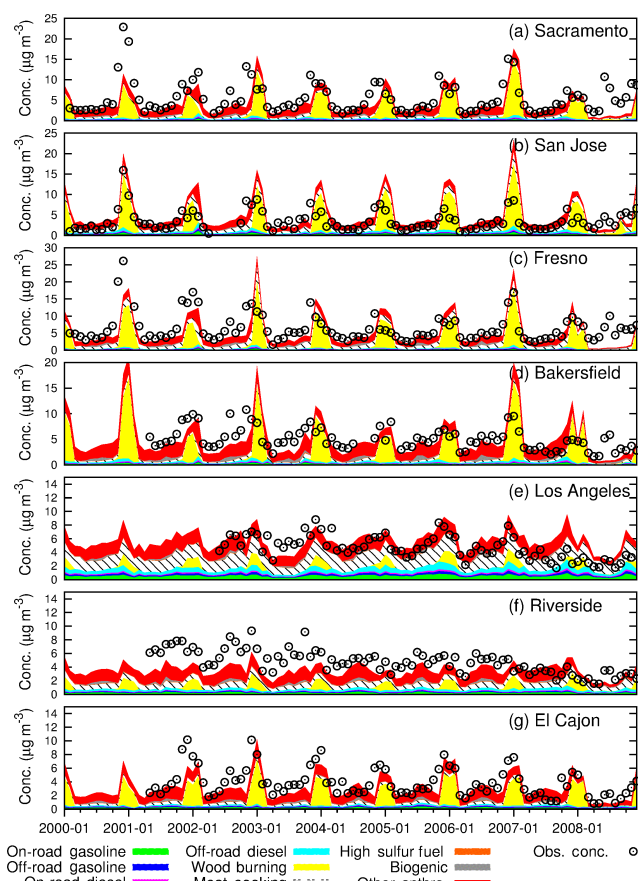


Figure 1. Monthly source contributions to $PM_{2.5}$ total OC at seven urban sites. Observed total OC concentrations are indicated by the circles with dots, and predicted OC concentrations from different sources are indicated by the colored areas.

heating fuels conducted by the Bay Area Air Quality Management District (BAAQMD). Model calculations generally underpredict OC in summer when concentrations are lower. Meat cooking and other anthropogenic sources are predicted to be the largest sources in summer at Sacramento, San Jose, Fresno, and Bakersfield. Together these two categories contribute over 86% of the total predicted OC in summer. Both measured and predicted seasonal variation is weaker at Los Angeles and Riverside than in Northern California due to smaller wood smoke contributions. Meat cooking and other anthropogenic sources make the largest predicted contributions to OA at these two Southern California locations. Mobile sources (gasoline and diesel engines) also contribute approximately 30% of the total $PM_{2.5}$ OC at Los Angeles. Model calculations tend to underpredict $PM_{2.5}$ OC concentrations in all seasons in 2000–2006 at Riverside (approximately 80 km downwind of the Los Angeles urban center). Intense emissions transported from the upwind Los Angeles areas along with the meteorology and topography enhances photo-oxidation of volatile organic compounds (VOCs) and

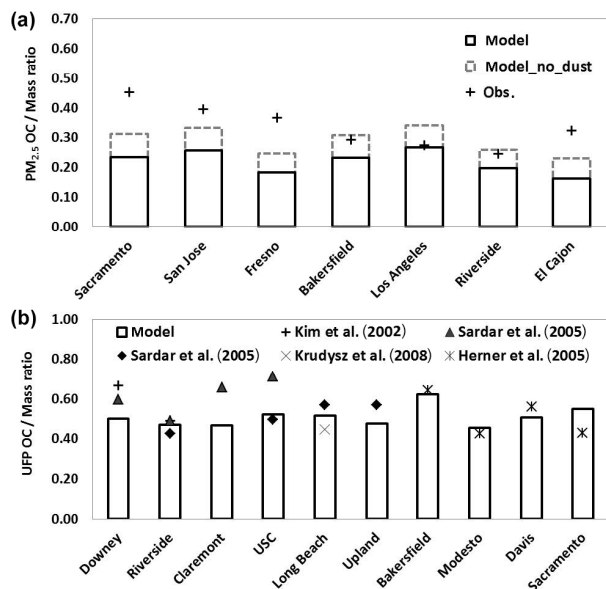


Figure 2. Observed (obs) and predicted (model) OC / mass ratios in (a) $PM_{2.5}$ and (b) ultrafine and quasi-ultrafine PM. In (a), a sensitivity analysis is conducted by removing the dust concentration from the $PM_{2.5}$ total mass (model_no_dust). The ultrafine and quasi-ultrafine data in (b) are extracted from published literature as indicated in the figure.

formation of SOA at this location. A measurement study of organic aerosols at Riverside in summer indicated high SOA fraction of the total OA (TOA) with an average SOA / OA ratio of 0.74 (Docherty et al., 2008). The $PM_{2.5}$ OC underprediction at Riverside during summer and the general underprediction in summer at other sites may indicate that some important precursors and pathways of $PM_{2.5}$ SOA are missing or only partially included in the current SOA module, such as SOA formation from glyoxal and methylglyoxal (Ervens and Volkamer, 2010; Fu et al., 2008; Ying et al., 2015) and from aerosol aqueous-phase chemistry (Volkamer et al., 2009), the conversion of intermediate-volatility compounds to SOA (Jathar et al., 2014; Zhao et al., 2014), or SOA forming with higher yields than included in the module (Zhang et al., 2014; Cappa et al., 2016).

Figure 2a compares the average $PM_{2.5}$ OC / mass ratios estimated from ambient measurements and the values predicted by the UCD/CIT model over the 9-year study period at seven representative urban locations. Predicted concentrations on the corresponding days were extracted and averaged for the comparison. The average OC / mass ratios were then calculated. The observed average OC / mass ratios vary in the range of 0.24 (at Riverside) to 0.45 (at Sacramento). The predicted average OC / mass ratios are in relatively good agreement with measured values at Los Angeles, Riverside, and Bakersfield (difference < 20 %) but not at Sacramento, San Jose, Fresno, and El Cajon (difference > 35 %). The predicted average OC / mass ratios are

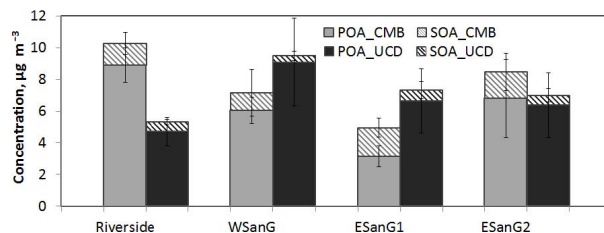


Figure 3. POA and SOA concentrations estimated by the CMB method (left gray columns) and predicted by the UCD/CIT model (right dark columns). Error bars represent the standard deviation of concentrations estimated during the sampling periods by both methods. The uncertainties of CMB-derived SOA range from 1 to 22 % (Daher et al., 2012). The data are for sampling periods in 2005–2007 at four sites in Southern California.

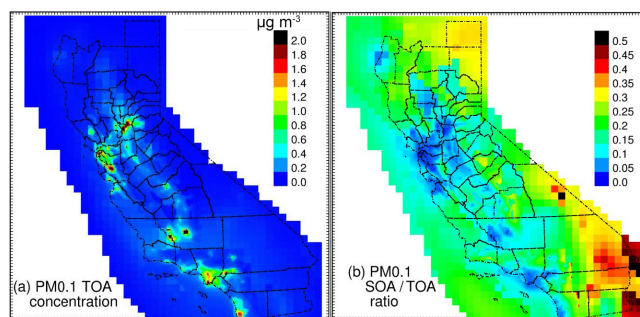


Figure 4. Predicted 9-year average (a) $PM_{0.1}$ total OA (TOA) concentration and (b) $PM_{0.1}$ SOA / TOA ratio in California.

consistently lower than observed ratios, by 0.01 (3 % at Los Angeles) to 0.22 (48 % at Sacramento). This underprediction is partly attributed to the underprediction of OC concentrations, especially the SOA concentrations, as well as to the overprediction of total mass concentrations due to overestimated dust emissions (Hu et al., 2014a, 2015). The seasonal average dust emissions used in the current study were not adjusted based on wind speed and soil moisture. A sensitivity analysis was conducted by removing the dust concentrations from the predicted $PM_{2.5}$ mass (Fig. 2a). The average predicted OC / mass ratio increased from 0.22 to 0.29 (average across the seven sites), compared to the observed ratio of 0.33. Omission of dust from the model predictions improves agreement with OC / mass measurements at all sites except central Los Angeles, although OC / mass without dust is still lower than measurements at four sites (Sacramento, San Jose, Fresno, and El Cajon), indicating OC predictions are likely biased low at these locations.

Figure 2b compares the predicted and observed OC / mass ratios in the ultrafine ($PM_{0.1}$) or quasi-ultrafine ($PM_{0.18}$, $PM_{0.25}$) particles. The ultrafine/quasi-ultrafine measurement data were compiled in a previous study (Hu et al., 2014a) from published literature (Herner et al., 2005; Kim et al., 2002; Krudysz et al., 2008; Sardar et al., 2005a, b). The ultrafine or quasi-ultrafine data are more sparse than the $PM_{2.5}$

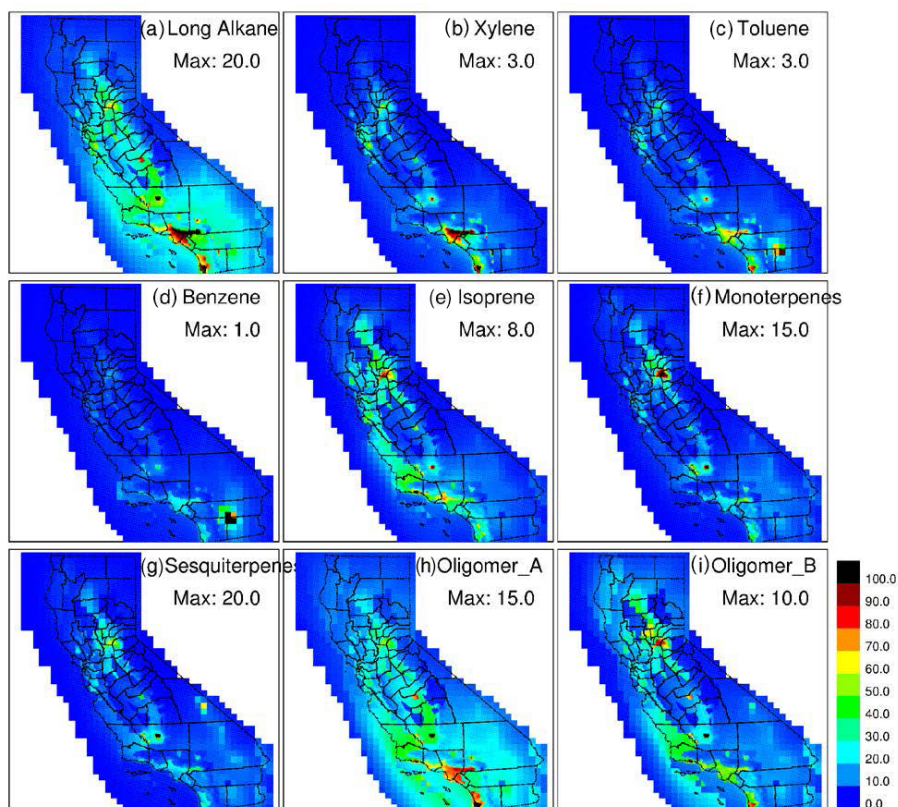


Figure 5. The 9-year average $\text{PM}_{0.1}$ SOA concentrations derived from (a) AALK, (b) AXYL, (c) ATOL, (d) ABNZ, (e) AISO, (f) ATRP, (g) ASQT, (h) AOLGA, and (i) AOLGB. Note that AXYL and ATOL are actually derived from lumped aromatics species ARO2 (groups of aromatics with $\text{kOH} > 2 \times 10^4 \text{ ppm}^{-1} \text{ min}^{-1}$, including xylenes and other di- and polyalkylbenzenes) and ARO1 (groups of aromatics with $\text{kOH} < 2 \times 10^4 \text{ ppm}^{-1} \text{ min}^{-1}$, including toluene and monoalkylbenzenes). The color scales (shown in the last panel in unit of %) indicate the ratios of the concentrations to the maximum 9-year average values, which are shown in the panels under species names with a unit of ng m^{-3} .

data, but they still cover a sufficient total number of days to allow for robust comparison. The observed OC/mass ratios in ultrafine/quasi-ultrafine sizes vary from 0.43 (at Modesto) to 0.71 (at USC). The predicted ultrafine/quasi-ultrafine OC/mass ratios generally agree well with observed values at all sites. The generally better agreement of OC/mass ratios in the ultrafine/quasi-ultrafine size range compared to the $\text{PM}_{2.5}$ size range reflects the fact that SOA formation and dust emissions make limited contributions to ultrafine/quasi-ultrafine concentrations. Condensation of the semivolatile products to form SOA mostly takes place in the particle accumulation mode and is generally not dominant in the ultrafine size range due to the increase in the saturation vapor pressure above small particles (Kelvin effect). Dust components mainly contribute to coarse and fine particles but make little contribution to the ultrafine particles.

The primary and secondary fraction of total OA cannot be directly measured in ambient OA samples. A few indirect methods have been developed to estimate the POA and SOA concentrations, such as molecular marker-based method (Daher et al., 2011, 2012; Ham and Kleeman, 2011; Kleindienst et al., 2007), elemental carbon (EC) tracer method (Cabada et

al., 2004; Lim et al., 2003; Polidori et al., 2006, 2007; Turpin and Huntzicker, 1995), water-soluble OC content method (Weber et al., 2007), aerosol mass spectrometry factorization method (Aiken et al., 2008; Lanz et al., 2007; Ulbrich et al., 2009), and the unexplained fraction of OA by tracers for major POA categories (Chen et al., 2010; Schauer and Cass, 2000). In the current study, $\text{PM}_{2.5}$ SOA concentrations were estimated by the molecular marker chemical mass balance (CMB) method (Daher et al., 2012) during sampling periods in 2005–2007 at four locations. $\text{PM}_{2.5}$ POA concentrations were then estimated by subtracting $\text{PM}_{2.5}$ SOA concentrations estimated by the CMB method from the total measured OA concentrations. Figure 3 shows the $\text{PM}_{2.5}$ POA and SOA concentrations predicted by the UCD/CIT model (right dark columns) compared to the $\text{PM}_{2.5}$ POA and SOA concentrations estimated using the CMB method (left gray columns). Error bars represent the standard deviation of concentrations estimated during the sampling periods. The total $\text{PM}_{2.5}$ OA (i.e., POA + SOA) concentrations predicted by the UCD/CIT model generally agree with measured values (with fractional bias within $\pm 35\%$) except at the Riverside site (with a fraction bias of -63%). However, the $\text{PM}_{2.5}$ SOA concentra-

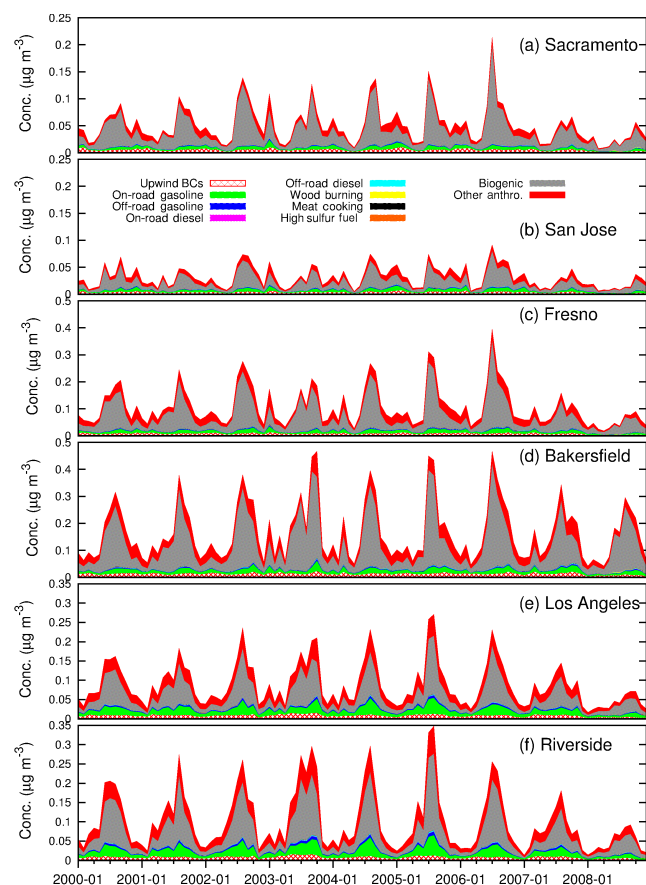


Figure 6. Monthly source contributions to $\text{PM}_{0.1}$ SOA at six urban sites. Predicted $\text{PM}_{0.1}$ SOA concentrations from different sources are indicated by the colored areas.

tions predicted by the UCD/CIT model appear to be a factor of 2–3 lower than the SOA concentrations estimated by the CMB method (ratio ranging from 2.2 at Riverside to 2.8 at WSanG). The $\text{PM}_{2.5}$ POA concentrations predicted by the UCD/CIT model are higher than those estimated by the CMB method at WSanG and ESanG1. This may reflect the effects of POA volatility. Studies have indicated that some fraction of POA emissions will evaporate, and this material may undergo photo-oxidation and condense back to particle phase (Robinson et al., 2007). In the current model, POA is treated as nonvolatile. Thus, no such evaporation occurs. However, the substantial underprediction of $\text{PM}_{2.5}$ SOA at all sites suggests that some SOA precursors and pathways are likely missing from the current SOA mechanism. Both $\text{PM}_{2.5}$ POA and SOA are underpredicted at Riverside, indicating that some important sources are likely missing in that area.

Figure 4 illustrates the predicted total $\text{PM}_{0.1}$ OA concentrations (Fig. 4a) and the predicted ratios of SOA to total OA averaged over the 9-year modeling period (Fig. 4b). High total $\text{PM}_{0.1}$ OA concentrations with maximum concentra-

tions $> 2 \mu\text{g m}^{-3}$ are located in urban areas where the POA emissions are large due to human activities. Predicted $\text{PM}_{0.1}$ SOA generally accounts for less than 10 % of total $\text{PM}_{2.5}$ OA at urban areas, but predicted SOA contribute to 10–20 % of total OA in suburban areas and to 20–50 % in rural areas. The spatial distribution of $\text{PM}_{2.5}$ SOA concentrations and the ratios of SOA to total OA in Fig. S1 in the Supplement) are generally similar to those of $\text{PM}_{0.1}$, but $\text{PM}_{0.1}$ OA has sharper spatial gradients and the $\text{PM}_{0.1}$ SOA fraction is lower than that in $\text{PM}_{2.5}$ in urban areas, indicating POA contributes more in the ultrafine size range.

Figure 5 shows the contributions from the nine precursor species to the $\text{PM}_{0.1}$ SOA concentrations (results of $\text{PM}_{2.5}$ SOA are shown in Fig. S2). Maximum SOA concentrations are located in southern part of the San Joaquin Valley (SJV). Monoterpenes, sesquiterpenes, oligomers, and long alkanes are the most important precursors, contributing over 90 % of the total SOA in most areas, while other precursors (xylene, toluene, and benzene) in total contribute less than 10 ng m^{-3} to SOA concentrations. These findings are very dependent on the treatment of vapor wall losses during the formulation of the SOA model. The contributions from different precursors to SOA concentrations have very different spatial distributions. Long-chain alkanes form SOA mainly in the urban areas of Southern California and in the middle-southern portion of the SJV. Isoprene, monoterpenes, and sesquiterpenes form SOA at coastal and foothill locations where the biogenic emissions are greatest. The longer lifetime of long-chain alkanes than isoprene leads to a broader spatial distribution for the SOA derived from alkanes. The spatial distribution of oligomers of anthropogenic SOA (Oligomer_A) and biogenic SOA (Oligomer_B) reflects the patterns of SOA derived from long-chain alkanes and the total biogenic species. The relative spatial patterns associated with each precursor are generally not sensitive to the exact formulation of the SOA model (see Sect. 3.3).

3.2 Sources of POA and SOA

Figure 6 displays the time series of monthly average $\text{PM}_{0.1}$ SOA source contributions at the six major urban locations. $\text{PM}_{0.1}$ SOA concentrations are high in summer ($100\text{--}300 \text{ ng m}^{-3}$) and low ($20\text{--}50 \text{ ng m}^{-3}$) in winter, reflecting the seasonal variation in photochemistry. $\text{PM}_{0.1}$ SOA concentrations are higher at Fresno and Bakersfield than other sites due to larger biogenic source contributions. Biogenic emissions are the largest source of $\text{PM}_{0.1}$ SOA across all sites, followed by the other anthropogenic sources (mainly solvent usage and waste disposal emissions, see Fig. S3). On-road gasoline engines are an important source of SOA at Los Angeles and Riverside. Similar source contributions to $\text{PM}_{2.5}$ SOA are found and shown in Fig. S4.

Figure 7 shows the predicted regional source contributions of $\text{PM}_{0.1}$ POA averaged over the 9-year modeling period. The important regional sources of $\text{PM}_{0.1}$ POA over the en-

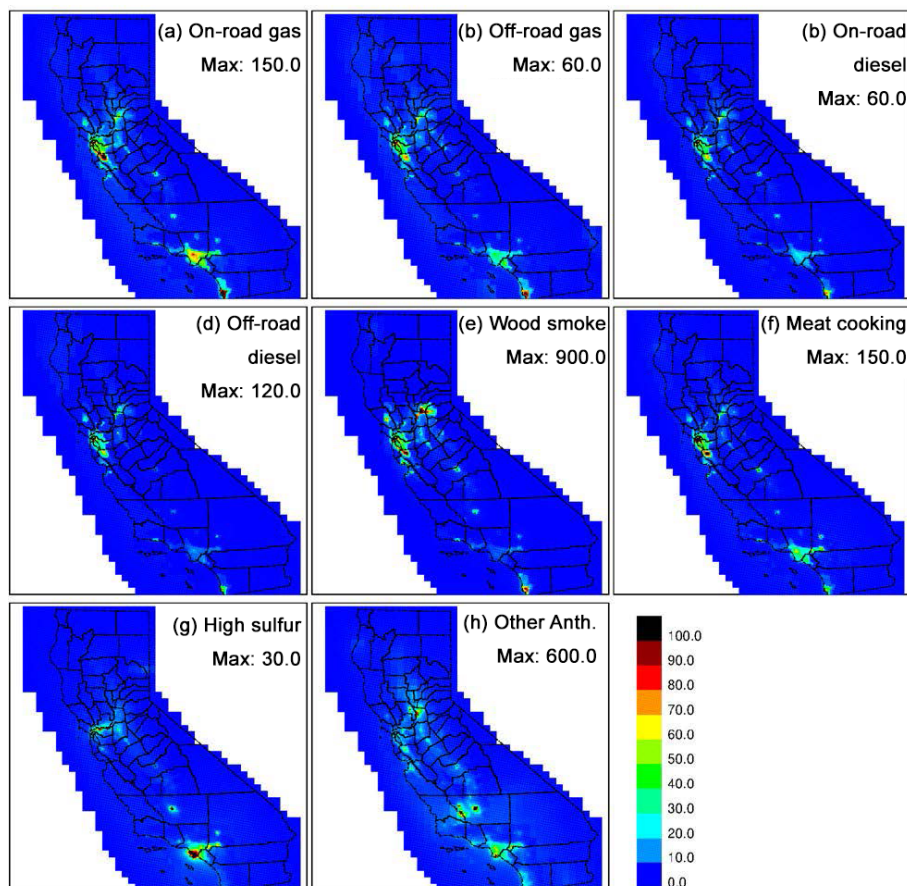


Figure 7. Predicted source contributions to 9-year average $\text{PM}_{0.1}$ POA concentrations. The color scales (shown in the last panel in unit of %) indicate the ratio of the concentrations to the maximum 9-year average concentration values, which are shown in the panels under source names with a unit of ng m^{-3} .

tirety of California are predicted to be other anthropogenic sources (contributing 39.6%), wood smoke (37.1%), on-road gasoline (9.1%), and meat cooking (5.8%). Wood smoke is the dominant POA source especially in Northern California, with the maximum $\text{PM}_{0.1}$ POA contribution exceeding $1 \mu\text{g m}^{-3}$. Meat cooking and mobile (on-road and off-road) sources are the major sources in urban areas, especially in metropolitan areas such as the Greater Los Angeles Area and the San Francisco Bay Area. Other anthropogenic sources from another major category in the urban centers in the SJV and also the Los Angeles areas. High-sulfur-content fuel sources are mainly located around the ports in the Los Angeles and San Francisco Bay areas. The regional source contributions of $\text{PM}_{0.1}$ POA are quite different from those of $\text{PM}_{2.5}$ POA (shown in Fig. S5). The $\text{PM}_{2.5}$ POA source contributions are much more widespread than the $\text{PM}_{0.1}$ POA sources contributions because $\text{PM}_{2.5}$ has a longer lifetime due to slower deposition and coagulation compared to $\text{PM}_{0.1}$. For example, the mobile sources and the other anthropogenic sources contribute greatly to $\text{PM}_{2.5}$ POA throughout the entire SJV but only contribute to $\text{PM}_{0.1}$ POA in urban centers.

Figure 8 shows the predicted regional source contributions of $\text{PM}_{0.1}$ SOA averaged over the 9-year modeling period (and Fig. S6 shows the $\text{PM}_{2.5}$ SOA results). Biogenic emission is predicted to be the single largest $\text{PM}_{0.1}$ SOA source in the present study, contributing 63.7% of the $\text{PM}_{0.1}$ SOA over the entire California. The maximum biogenic $\text{PM}_{0.1}$ SOA concentration is up to $0.1 \mu\text{g m}^{-3}$ around Bakersfield in the southern SJV. Other anthropogenic sources (22.2%) and on-road gasoline engines (10.8%) are predicted to be the most important anthropogenic sources of $\text{PM}_{0.1}$ SOA in California. The spatial distribution of $\text{PM}_{0.1}$ SOA concentrations from these anthropogenic sources are similar (but different from the spatial distribution of SOA from biogenic sources) with high concentrations in Southern California. $\text{PM}_{0.1}$ SOA formation from on-road diesel engines, off-road diesel engines, wood smoke, meat cooking, and high-sulfur fuel combustion are small, with $\text{PM}_{0.1}$ SOA contributions generally less than a few ng m^{-3} . A recent epidemiological study has revealed that anthropogenic $\text{PM}_{0.1}$ SOA is highly associated with ischemic heart disease mortality (Ostro et al., 2015). Therefore, the results in this study suggest that control of sol-

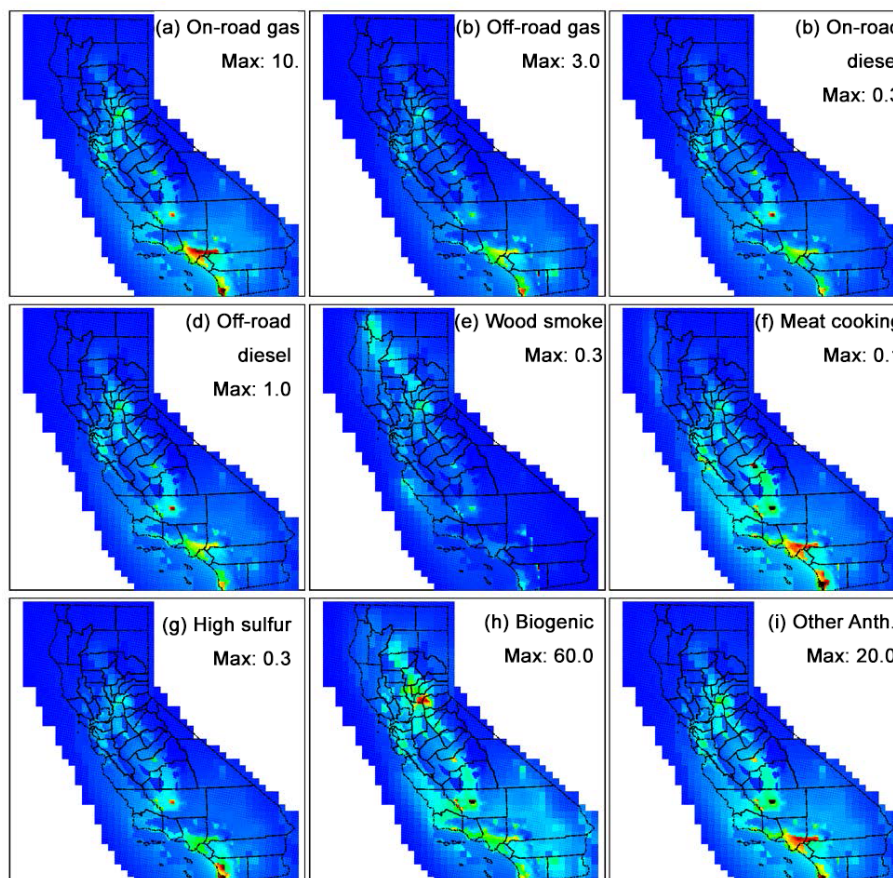


Figure 8. Predicted source contributions to 9-year average $\text{PM}_{0.1}$ SOA concentrations. The definition of the color scales is the same as in Fig. 7.

vent usage, waste disposal, and mobile emissions should be considered to protect public health in California, but the exact determination of source controls will need to be evaluated after the SOA formation mechanism is updated.

3.3 Influence of vapor wall losses on SOA exposure in California

The SOA concentrations predicted in the current study are based on the SOA yield data measured in chamber experiments. A recent study has demonstrated that organic vapors can be lost to chamber walls during SOA formation experiments, resulting in SOA yields that are biased low (Zhang et al., 2014). Efforts have been carried out to parameterize the effect of vapor wall losses on SOA formation in the UCD/CIT air quality model to account for this effect when predicting ambient SOA concentrations in Southern California (Cappa et al., 2016). SOA concentrations are predicted to increase by factors of 2–5 with low vapor wall loss rates and by factors of 5–10 with high vapor wall loss rates compared to the concentrations in the simulations with no consideration of vapor wall losses. Due to low SOA / TOA frac-

tions (< 10 %) at the observation sites located in urban areas (Figs. 4 and S1), the substantial increase of SOA by the vapor wall loss corrections does not strongly change the total OA concentrations and therefore does not significantly affect the model evaluation results shown in Fig. 1. Here we further analyzed the changes in the population weighted concentrations (PWCs) of SOA when vapor wall losses are accounted for. Two sets of simulations (scenarios) conducted by Cappa et al. (2016) are considered, one with the low- NO_x , high-yield parameters (denoted as “highyield”) and the other with high- NO_x , low-yield parameters (denoted as “lowyield”). Each set of simulations included three vapor wall loss cases, i.e., no consideration of vapor wall losses (denoted as “base”), low vapor wall loss rates (denoted as “lowwallloss”), and high vapor wall loss rates (denoted as “highwallloss”). PWCs of SOA are calculated for six counties in the Southern California for the six scenarios. Spatial difference in exposure is important in cohort studies; therefore the relative changes of PWCs among counties are examined. Figure 9 shows the PWCs of SOA and their relative changes in different scenarios in the six counties. The results indicate that PWCs of SOA increase substantially by accounting for vapor wall

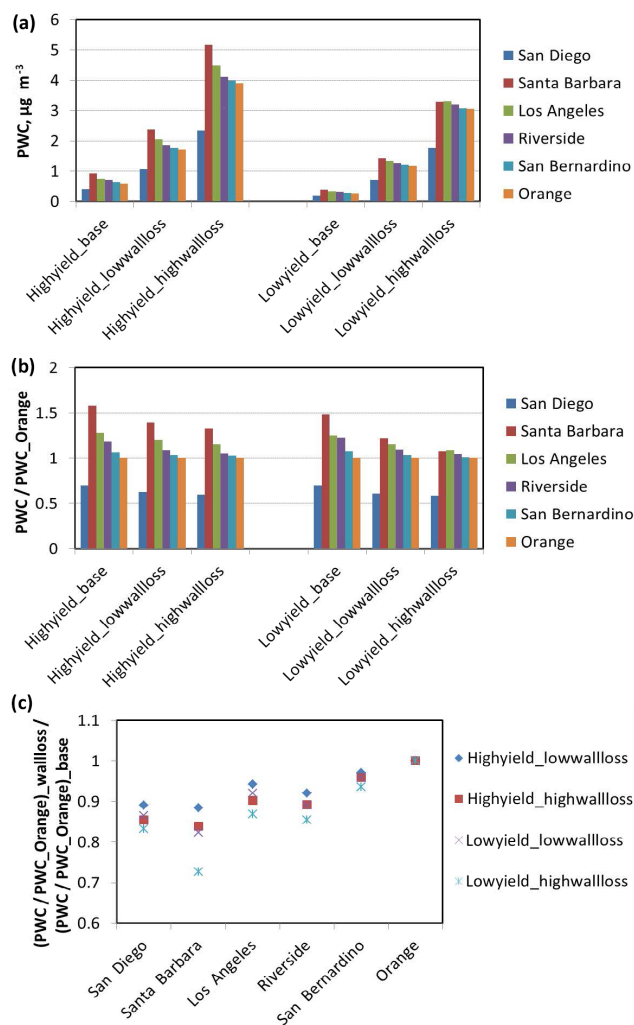


Figure 9. (a) Predicted population weighted concentrations (PWCs) of SOA in six counties in Southern California. Two sets of simulations (scenarios) conducted by Cappa et al. (2016) were used, one with the low- NO_x , high-yield parameters (denoted as “high-yield”) and the other with high- NO_x , low-yield parameters (denoted as “lowyield”). Each set of simulations included three vapor wall loss cases, i.e., no considering of vapor wall losses (denoted as “base”), low vapor wall loss rates (denoted as “lowwallloss”), and high vapor wall loss rates (denoted as “highwallloss”). (b) Normalized PWCs of SOA in all counties to the PWC of SOA in Orange County. (c) Changes in the normalized PWCs of SOA in all counties by accounting for vapor wall losses.

losses in all counties (panel a). However, the spatial pattern of SOA PWC, as characterized by normalizing the PWC for each location by the PWC in Orange County, is very similar in all scenarios (panel b). Consequently, accounting for vapor wall losses changes the SOA exposure ratio in different counties by only a small extent of $< 15\%$ for most scenarios/counties (panel c). These results suggest that future simulations that account for vapor wall losses in SOA simu-

lations will yield increased absolute values of concentrations but will have spatial patterns that are similar to the base case results in the current paper when used for epidemiology studies.

Figure 9 suggests that associations between anthropogenic SOA and health effects identified in previous epidemiological studies will prove robust to future updates in SOA models. This finding also extends to the spatial pattern of individual SOA precursors. The influence of vapor wall losses on exposure to SOA formed from different precursors (i.e., long alkanes, aromatics, isoprene, sesquiterpenes, and monoterpenes) is shown in Figs. S7–S11. In all cases, the spatial pattern of PWC for SOA derived from each precursor is similar under all treatments of wall losses. Long alkanes and aromatics are mainly from anthropogenic sources, and isoprene, sesquiterpenes, and monoterpenes are mostly from biogenic sources. Further detailed interpretation of source contributions to SOA and associated health effects should only be carried out after new exposure fields are calculated using the latest SOA models.

4 Conclusions

The source-oriented UCD/CIT model was applied to predict the concentrations and sources of $\text{PM}_{0.1}$ POA and SOA in California for a 9-year (2000–2008) modeling period with 4 km horizontal resolution to provide data for health effect studies. As a confidence-building measure, predicted total $\text{PM}_{2.5}$ OC concentrations (primary + secondary) and the $\text{PM}_{2.5}$ and $\text{PM}_{0.1}$ OC / mass ratios generally agree with measured values at fixed point locations. Compared to the POA and SOA concentrations estimated from measurements at four sites using the CMB method, the $\text{PM}_{2.5}$ total OA concentrations predicted by the UCD/CIT model have a fractional bias within $\pm 35\%$ except at the Riverside site. The CMB model estimated $\text{PM}_{2.5}$ SOA concentrations accounted for 13–37% of total OA while the UCD/CIT SOA concentrations accounted for 4–11% of total OA. POA volatility, incomplete SOA formation mechanism, and/or missing sources may account for the discrepancy. For these reasons, the current study focuses on the $\text{PM}_{0.1}$ size fraction.

$\text{PM}_{0.1}$ OA has larger contributions from primary sources than the $\text{PM}_{2.5}$ size fraction. Wood smoke is found to be the single biggest source of $\text{PM}_{0.1}$ OA in winter in California and meat cooking, mobile sources, and other anthropogenic sources (mainly solvent usage and waste disposal) are the most important sources in summer, but these rankings are sensitive to the SOA model used in the calculation. Biogenic emissions are predicted to be the largest $\text{PM}_{0.1}$ SOA source, followed by the other anthropogenic sources and mobile sources. A recent epidemiological study has revealed that anthropogenic $\text{PM}_{0.1}$ SOA is highly associated with ischemic heart disease mortality (Ostro et al., 2015). Therefore, the results in the present study suggest that control of

solvent usage, waste disposal, and mobile emissions should be considered to protect public health in California, but detailed source control programs can only be carried out after revised calculations are performed using updated SOA models. The predicted spatial distributions of the concentrations and sources of POA and SOA in $PM_{0.1}$ over the 9-year periods provide detailed information for epidemiological studies to further investigate the associations with other health outcomes, and these spatial patterns are generally not sensitive to the treatment of wall losses in the SOA model formulation.

Data availability. All model results included in the current paper can be downloaded free of charge at <http://faculty.engineering.ucdavis.edu/kleeman/>

The Supplement related to this article is available online at doi:10.5194/acp-17-5379-2017-supplement.

Competing interests. The authors declare that they have no conflict of interest.

Acknowledgements. This study was funded by the United States Environmental Protection Agency under grant no. R83386401. Although the research described in the article has been funded by the United States Environmental Protection Agency it has not been subject to the agency's required peer and policy review and therefore does not necessarily reflect the reviews of the agency and no official endorsement should be inferred.

Edited by: Q. Zhang

Reviewed by: three anonymous referees

References

- Aiken, A. C., DeCarlo, P. F., Kroll, J. H., Worsnop, D. R., Huffman, J. A., Docherty, K. S., Ulbrich, I. M., Mohr, C., Kimmel, J. R., Sueper, D., Sun, Y., Zhang, Q., Trimborn, A., Northway, M., Ziemann, P. J., Canagaratna, M. R., Onasch, T. B., Alfarra, M. R., Prevot, A. S. H., Dommen, J., Duplissy, J., Metzger, A., Baltensperger, U., and Jimenez, J. L.: O/C and OM/OC Ratios of Primary, Secondary, and Ambient Organic Aerosols with High-Resolution Time-of-Flight Aerosol Mass Spectrometry, *Environ. Sci. Technol.*, 42, 4478–4485, 2008.
- Boylan, J. W. and Russell, A. G.: PM and light extinction model performance metrics, goals, and criteria for three-dimensional air quality models, *Atmos. Environ.*, 40, 4946–4959, 2006.
- Cabada, J. C., Pandis, S. N., Subramanian, R., Robinson, A. L., Polidori, A., and Turpin, B.: Estimating the secondary organic aerosol contribution to $PM_{2.5}$ using the EC tracer method, *Aerosol Sci. Tech.*, 38, 140–155, 2004.
- Cao, J. J., Xu, H. M., Xu, Q., Chen, B. H., and Kan, H. D.: Fine Particulate Matter Constituents and Cardiopulmonary Mortality in a Heavily Polluted Chinese City, *Environ. Health Persp.*, 120, 373–378, 2012.
- Cappa, C. D., Jathar, S. H., Kleeman, M. J., Docherty, K. S., Jimenez, J. L., Seinfeld, J. H., and Wexler, A. S.: Simulating secondary organic aerosol in a regional air quality model using the statistical oxidation model – Part 2: Assessing the influence of vapor wall losses, *Atmos. Chem. Phys.*, 16, 3041–3059, doi:10.5194/acp-16-3041-2016, 2016.
- CARB: Database: California Air Quality Data – Selected Data, available at: <http://www.arb.ca.gov/aqd/aqcd/aqcdcdld.htm> (last access: October 2016), 2011.
- Carlton, A. G., Bhawe, P. V., Napelenok, S. L., Edney, E. D., Sarwar, G., Pinder, R. W., Pouliot, G. A., and Houyoux, M.: Model Representation of Secondary Organic Aerosol in CMAQv4.7, *Environ. Sci. Technol.*, 44, 8553–8560, 2010.
- Chen, J. J., Ying, Q., and Kleeman, M. J.: Source apportionment of wintertime secondary organic aerosol during the California regional $PM_{10}/PM_{2.5}$ air quality study, *Atmos. Environ.*, 44, 1331–1340, 2010.
- Daher, N., Ruprecht, A., Invernizzi, G., De Marco, C., Miller-Schulze, J., Heo, J. B., Shafer, M. M., Schauer, J. J., and Sioutas, C.: Chemical Characterization and Source Apportionment of Fine and Coarse Particulate Matter Inside the Refectory of Santa Maria Delle Grazie Church, Home of Leonardo Da Vinci's "Last Supper", *Environ. Sci. Technol.*, 45, 10344–10353, 2011.
- Daher, N., Ruprecht, A., Invernizzi, G., De Marco, C., Miller-Schulze, J., Heo, J. B., Shafer, M. M., Shelton, B. R., Schauer, J. J., and Sioutas, C.: Characterization, sources and redox activity of fine and coarse particulate matter in Milan, Italy, *Atmos. Environ.*, 49, 130–141, 2012.
- Docherty, K. S., Stone, E. A., Ulbrich, I. M., DeCarlo, P. F., Snyder, D. C., Schauer, J. J., Peltier, R. E., Weber, R. J., Murphy, S. M., Seinfeld, J. H., Grover, B. D., Eatough, D. J., and Jimenez, J. L.: Apportionment of Primary and Secondary Organic Aerosols in Southern California during the 2005 Study of Organic Aerosols in Riverside (SOAR-1), *Environ. Sci. Technol.*, 42, 7655–7662, 2008.
- Dockery, D. W.: Epidemiologic evidence of cardiovascular effects of particulate air pollution, *Environ. Health Persp.*, 109, 483–486, 2001.
- Dockery, D. W. and Pope, C. A.: Acute Respiratory Effects of Particulate Air-Pollution, *Annu. Rev. Publ. Health*, 15, 107–132, 1994.
- Dockery, D. W., Pope, C. A., Xu, X. P., Spengler, J. D., Ware, J. H., Fay, M. E., Ferris, B. G., and Speizer, F. E.: An Association between Air-Pollution and Mortality in 6 United-States Cities, *New Engl. J. Med.*, 329, 1753–1759, 1993.
- Ervens, B. and Volkamer, R.: Glyoxal processing by aerosol multiphase chemistry: towards a kinetic modeling framework of secondary organic aerosol formation in aqueous particles, *Atmos. Chem. Phys.*, 10, 8219–8244, doi:10.5194/acp-10-8219-2010, 2010.
- Franklin, M., Zeka, A., and Schwartz, J.: Association between $PM_{2.5}$ and all-cause and specific-cause mortality in 27 US communities, *J. Expo. Sci. Env. Epid.*, 17, 279–287, 2007.
- Fu, T. M., Jacob, D. J., Wittrock, F., Burrows, J. P., Vrekoussis, M., and Henze, D. K.: Global budgets of atmospheric glyoxal and methylglyoxal, and implications for formation of sec-

- ondary organic aerosols, *J. Geophys. Res.-Atmos.*, 113, D15303, doi:10.1029/2007JD009505, 2008.
- Ham, W. A. and Kleeman, M. J.: Size-resolved source apportionment of carbonaceous particulate matter in urban and rural sites in central California, *Atmos. Environ.*, 45, 3988–3995, 2011.
- Herner, J. D., Aw, J., Gao, O., Chang, D. P., and Kleeman, M. J.: Size and composition distribution of airborne particulate matter in northern California: I-particulate mass, carbon, and water-soluble ions, *J. Air Waste Manage.*, 55, 30–51, 2005.
- Hu, J., Ying, Q., Chen, J. J., Mahmud, A., Zhao, Z., Chen, S. H., and Kleeman, M. J.: Particulate air quality model predictions using prognostic vs. diagnostic meteorology in central California, *Atmos. Environ.*, 44, 215–226, 2010.
- Hu, J., Howard, C. J., Mitloehner, F., Green, P. G., and Kleeman, M. J.: Mobile Source and Livestock Feed Contributions to Regional Ozone Formation in Central California, *Environ. Sci. Technol.*, 46, 2781–2789, 2012.
- Hu, J., Zhang, H., Chen, S.-H., Vandenberghe, F., Ying, Q., and Kleeman, M. J.: Predicting Primary PM_{2.5} and PM_{0.1} Trace Composition for Epidemiological Studies in California, *Environ. Sci. Technol.*, 48, 4971–4979, 2014a.
- Hu, J., Zhang, H., Chen, S., Ying, Q., Vandenberghe, F., and Kleeman, M. J.: Identifying PM_{2.5} and PM_{0.1} Sources for Epidemiological Studies in California, *Environ. Sci. Technol.*, 48, 4980–4990, 2014b.
- Hu, J., Zhang, H., Ying, Q., Chen, S.-H., Vandenberghe, F., and Kleeman, M. J.: Long-term particulate matter modeling for health effect studies in California – Part I: Model performance on temporal and spatial variations, *Atmos. Chem. Phys.*, 15, 3445–3461, doi:10.5194/acp-15-3445-2015, 2015.
- Jathar, S. H., Gordon, T. D., Hennigan, C. J., Pye, H. O. T., Pouliot, G., Adams, P. J., Donahue, N. M., and Robinson, A. L.: Unspecified organic emissions from combustion sources and their influence on the secondary organic aerosol budget in the United States, *P. Natl. Acad. Sci. USA*, 111, 10473–10478, 2014.
- Jathar, S. H., Mahmud, A., Barsanti, K. C., Asher, W. E., Pankow, J. F., and Kleeman, M. J.: Water uptake by organic aerosol and its influence on gas/particle partitioning of secondary organic aerosol in the United States, *Atmos. Environ.*, 129, 142–154, 2016.
- Kim, S., Shen, S., Sioutas, C., Zhu, Y. F., and Hinds, W. C.: Size distribution and diurnal and seasonal trends of ultrafine particles in source and receptor sites of the Los Angeles basin, *J. Air Waste Manage.*, 52, 297–307, 2002.
- Kleeman, M. J., Ying, Q., Lu, J., Mysliwicz, M. J., Griffin, R. J., Chen, J. J., and Clegg, S.: Source apportionment of secondary organic aerosol during a severe photochemical smog episode, *Atmos. Environ.*, 41, 576–591, 2007.
- Kleeman, M. J., Riddle, S. G., Robert, M. A., Jakober, C. A., Fine, P. M., Hays, M. D., Schauer, J. J., and Hannigan, M. P.: Source Apportionment of Fine (PM_{1.8}) and Ultrafine (PM_{0.1}) Airborne Particulate Matter during a Severe Winter Pollution Episode, *Environ. Sci. Technol.*, 43, 272–279, 2009.
- Kleindienst, T. E., Jaoui, M., Lewandowski, M., Offenber, J. H., Lewis, C. W., Bhave, P. V., and Edney, E. O.: Estimates of the contributions of biogenic and anthropogenic hydrocarbons to secondary organic aerosol at a southeastern US location, *Atmos. Environ.*, 41, 8288–8300, 2007.
- Krall, J. R., Anderson, G. B., Dominici, F., Bell, M. L., and Peng, R. D.: Short-term Exposure to Particulate Matter Constituents and Mortality in a National Study of US Urban Communities, *Environ. Health Persp.*, 121, 1148–1153, 2013.
- Krudysz, M. A., Froines, J. R., Fine, P. M., and Sioutas, C.: Intra-community spatial variation of size-fractionated PM mass, OC, EC, and trace elements in the Long Beach, CA area, *Atmos. Environ.*, 42, 5374–5389, 2008.
- Lanz, V. A., Wacker, L., Weimer, S., Caseiro, A., Puxbaum, H., and Prevot, A. S. H.: Source Attribution of Submicron Organic Aerosols during Wintertime Inversions by Advanced Factor Analysis of Aerosol Mass Spectra, *Environ. Sci. Technol.*, 42, 214–220, 2007.
- Laurent, O., Hu, J. L., Li, L. F., Cockburn, M., Escobedo, L., Kleeman, M. J., and Wu, J.: Sources and contents of air pollution affecting term low birth weight in Los Angeles County, California, 2001–2008, *Environ. Res.*, 134, 488–495, 2014.
- Laurent, O., Hu, J., Li, L., Kleeman, M. J., Bartell, S. M., Cockburn, M., Escobedo, L., and Wu, J.: Low birth weight and air pollution in California: Which sources and components drive the risk?, *Environ. Int.*, 92–93, 471–477, 2016a.
- Laurent, O., Hu, J. L., Li, L. F., Kleeman, M. J., Bartell, S. M., Cockburn, M., Escobedo, L., and Wu, J.: A Statewide Nested Case-Control Study of Preterm Birth and Air Pollution by Source and Composition: California, 2001–2008, *Environ. Health Persp.*, 124, 1479–1486, doi:10.1289/ehp.1510133, 2016b.
- Le Tertre, A., Medina, S., Samoli, E., Forsberg, B., Michelozzi, P., Boumghar, A., Vonk, J. M., Bellini, A., Atkinson, R., Ayres, J. G., Sunyer, J., Schwartz, J., and Katsouyanni, K.: Short-term effects of particulate air pollution on cardiovascular diseases in eight European cities, *J. Epidemiol. Commun. H.*, 56, 773–779, 2002.
- Levy, J. I., Diez, D., Dou, Y. P., Barr, C. D., and Dominici, F.: A Meta-Analysis and Multisite Time-Series Analysis of the Differential Toxicity of Major Fine Particulate Matter Constituents, *Am. J. Epidemiol.*, 175, 1091–1099, 2012.
- Lim, H. J., Turpin, B. J., Russell, L. M., and Bates, T. S.: Organic and elemental carbon measurements during ACE-Asia suggest a longer atmospheric lifetime for elemental carbon, *Environ. Sci. Technol.*, 37, 3055–3061, 2003.
- Liu, Y., Bourgeois, A., Warner, T., Swerdlin, S., and Hacker, J.: An implementation of obs-nudging-based FDDA into WRF for supporting ATEC test operations, 2005 WRF user workshop, Paper 10.7, 2005.
- Mar, T. F., Norris, G. A., Koenig, J. Q., and Larson, T. V.: Associations between air pollution and mortality in Phoenix, 1995–1997, *Environ. Health Persp.*, 108, 347–353, 2000.
- Mauderly, J. L. and Chow, J. C.: Health effects of organic aerosols, *Inhal. Toxicol.*, 20, 257–288, 2008.
- Mysliwicz, M. J. and Kleeman, M. J.: Source apportionment of secondary airborne particulate matter in a polluted atmosphere, *Environ. Sci. Technol.*, 36, 5376–5384, 2002.
- Ostro, B., Broadwin, R., Green, S., Feng, W. Y., and Lipsett, M.: Fine particulate air pollution and mortality in nine California counties: Results from CALFINE, *Environ. Health Persp.*, 114, 29–33, 2006.
- Ostro, B., Lipsett, M., Reynolds, P., Goldberg, D., Hertz, A., Garcia, C., Henderson, K. D., and Bernstein, L.: Long-Term Exposure to

- Constituents of Fine Particulate Air Pollution and Mortality: Results from the California Teachers Study, *Environ. Health Persp.*, 118, 363–369, 2010.
- Ostro, B., Hu, J., Goldberg, D., Reynolds, P., Hertz, A., Bernstein, L., and Kleeman, M. J.: Associations of Mortality with Long-Term Exposures to Fine and Ultrafine Particles, Species and Sources: Results from the California Teachers Study Cohort, *Environ. Health Persp.*, 123, 549–556, doi:10.1289/ehp.1408565, 2015.
- Pankow, J. F., Marks, M. C., Barsanti, K. C., Mahmud, A., Asher, W. E., Li, J. Y., Ying, Q., Jathar, S. H., and Kleeman, M. J.: Molecular view modeling of atmospheric organic particulate matter: Incorporating molecular structure and co-condensation of water, *Atmos. Environ.*, 122, 400–408, 2015.
- Polidori, A., Turpin, B. J., Lim, H. J., Cabada, J. C., Subramanian, R., Pandis, S. N., and Robinson, A. L.: Local and regional secondary organic aerosol: Insights from a year of semi-continuous carbon measurements at Pittsburgh, *Aerosol Sci. Tech.*, 40, 861–872, 2006.
- Polidori, A., Arhami, M., Sioutas, C., Delfino, R. J., and Allen, R.: Indoor/Outdoor Relationships, Trends, and Carbonaceous Content of Fine Particulate Matter in Retirement Homes of the Los Angeles Basin, *J. Air Waste Manage.*, 57, 366–379, 2007.
- Pope, C. A. and Dockery, D. W.: Health effects of fine particulate air pollution: Lines that connect, *J. Air Waste Manage.*, 56, 709–742, 2006.
- Pope, C. A., Burnett, R. T., Thun, M. J., Calle, E. E., Krewski, D., Ito, K., and Thurston, G. D.: Lung cancer, cardiopulmonary mortality, and long-term exposure to fine particulate air pollution, *Jama-J. Am. Med. Assoc.*, 287, 1132–1141, 2002.
- Robinson, A. L., Donahue, N. M., Shrivastava, M. K., Weitkamp, E. A., Sage, A. M., Grieshop, A. P., Lane, T. E., Pierce, J. R., and Pandis, S. N.: Rethinking Organic Aerosols: Semivolatile Emissions and Photochemical Aging, *Science*, 315, 1259–1262, 2007.
- Sardar, S. B., Fine, P. M., and Sioutas, C.: Seasonal and spatial variability of the size-resolved chemical composition of particulate matter (PM₁₀) in the Los Angeles Basin, *J. Geophys. Res.-Atmos.*, 110, D07S08, doi:10.1029/2004JD004627, 2005a.
- Sardar, S. B., Fine, P. M., Mayo, P. R., and Sioutas, C.: Size-fractionated measurements of ambient ultrafine particle chemical composition in Los Angeles using the NanoMOUDI, *Environ. Sci. Technol.*, 39, 932–944, 2005b.
- Schauer, J. J. and Cass, G. R.: Source apportionment of wintertime gas-phase and particle-phase air pollutants using organic compounds as tracers, *Environ. Sci. Technol.*, 34, 1821–1832, 2000.
- Seinfeld, J. H. and Pankow, J. F.: Organic atmospheric particulate material, *Annu. Rev. Phys. Chem.*, 54, 121–140, 2003.
- Turpin, B. J. and Huntzicker, J. J.: Identification of Secondary Organic Aerosol Episodes and Quantitation of Primary and Secondary Organic Aerosol Concentrations during Scaqs, *Atmos. Environ.*, 29, 3527–3544, 1995.
- Turpin, B. J. and Lim, H. J.: Species contributions to PM_{2.5} mass concentrations: revisiting common assumptions for estimating organic mass, *Aerosol Sci. Tech.*, 35, 602–610, 2010.
- Ulbrich, I. M., Canagaratna, M. R., Zhang, Q., Worsnop, D. R., and Jimenez, J. L.: Interpretation of organic components from Positive Matrix Factorization of aerosol mass spectrometric data, *Atmos. Chem. Phys.*, 9, 2891–2918, doi:10.5194/acp-9-2891-2009, 2009.
- Volkamer, R., Ziemann, P. J., and Molina, M. J.: Secondary Organic Aerosol Formation from Acetylene (C₂H₂): seed effect on SOA yields due to organic photochemistry in the aerosol aqueous phase, *Atmos. Chem. Phys.*, 9, 1907–1928, doi:10.5194/acp-9-1907-2009, 2009.
- Weber, R. J., Sullivan, A. P., Peltier, R. E., Russell, A., Yan, B., Zheng, M., de Gouw, J., Warneke, C., Brock, C., Holloway, J. S., Atlas, E. L., and Edgerton, E.: A study of secondary organic aerosol formation in the anthropogenic-influenced southeastern United States, *J. Geophys. Res.-Atmos.*, 112, D13302, doi:10.1029/2007JD008408, 2007.
- William, C., Skamarock, J. B. K., Dudhia, J., Gill, D. O., Barker, D. M., Duda, M. G., Huang, X. Y., Wang, W., and Powers, J. G.: A Description of the Advanced Research WRF Version 3, NCAR Technical Note NCAR/TN-475+STR, June 2008.
- Ying, Q. and Kleeman, M. J.: Efficient Source Apportionment of Airborne Particulate Matter Using an Internally Mixed Air Quality Model with Artificial Tracers, *Environ. Sci. Eng. (China)*, 1, 91–99, 2004.
- Ying, Q. and Kleeman, M. J.: Source contributions to the regional distribution of secondary particulate matter in California, *Atmos. Environ.*, 40, 736–752, 2006.
- Ying, Q., Lu, J., Kaduwela, A., and Kleeman, M.: Modeling air quality during the California Regional PM₁₀/PM_{2.5} Air Quality Study (CPRAQS) using the UCD/CIT Source Oriented Air Quality Model – Part II. Regional source apportionment of primary airborne particulate matter, *Atmos. Environ.*, 42, 8967–8978, 2008.
- Ying, Q., Li, J., and Kota, S. H.: Significant Contributions of Isoprene to Summertime Secondary Organic Aerosol in Eastern United States, *Environ. Sci. Technol.*, 49, 7834–7842, 2015.
- Zhang, H. L. and Ying, Q.: Source apportionment of airborne particulate matter in Southeast Texas using a source-oriented 3D air quality model, *Atmos. Environ.*, 44, 3547–3557, 2010.
- Zhang, H. and Ying, Q.: Secondary organic aerosol formation and source apportionment in Southeast Texas, *Atmos. Environ.*, 45, 3217–3227, 2011.
- Zhang, Q., Jimenez, J. L., Canagaratna, M. R., Allan, J. D., Coe, H., Ulbrich, I., Alfarra, M. R., Takami, A., Middlebrook, A. M., Sun, Y. L., Dzepina, K., Dunlea, E., Docherty, K., DeCarlo, P. F., Salcedo, D., Onasch, T., Jayne, J. T., Miyoshi, T., Shimojo, A., Hatakeyama, S., Takegawa, N., Kondo, Y., Schneider, J., Drewnick, F., Borrmann, S., Weimer, S., Demerjian, K., Williams, P., Bower, K., Bahreini, R., Cottrell, L., Griffin, R. J., Rautiainen, J., Sun, J. Y., Zhang, Y. M., and Worsnop, D. R.: Ubiquity and dominance of oxygenated species in organic aerosols in anthropogenically-influenced Northern Hemisphere midlatitudes, *Geophys. Res. Lett.*, 34, L13801, doi:10.1029/2007GL029979, 2007.
- Zhang, X., Cappa, C. D., Jathar, S. H., Mcvay, R. C., Ensberg, J. J., Kleeman, M. J., and Seinfeld, J. H.: Influence of vapor wall loss in laboratory chambers on yields of secondary organic aerosol, *P. Natl. Acad. Sci. USA*, 111, 5802–5807, 2014.
- Zhao, Y. L., Hennigan, C. J., May, A. A., Tkacik, D. S., de Gouw, J. A., Gilman, J. B., Kuster, W. C., Borbon, A., and Robinson, A. L.: Intermediate-Volatility Organic Compounds: A Large Source of Secondary Organic Aerosol, *Environ. Sci. Technol.*, 48, 13743–13750, 2014.